T · H · E
OHIO
STATE
UNIVERSITY

Moment Method Analysis of the Electric Shielding Factor of a Conducting TM Shield at ELF

E.H. Newman and M. Kragalott

The Ohio State University

ElectroScience Laboratory

Department of Electrical Engineering
Columbus, Ohio 43212

Technical Report 721566-4
Contract No. N00014-89-J-1007 P00008
April 1995

Department of the Navy
Office of Naval Research
800 N. Quincy Street
Arlington, Virginia 22217-5000

NOTICES

When Government drawings, specifications, or other data are used for any purpose other than in connection with a definitely related Government procurement operation, the United States Government thereby incurs no responsibility nor any obligation whatsoever, and the fact that the Government may have formulated, furnished, or in any way supplied the said drawings, specifications, or other data, is not to be regarded by implication or otherwise as in any manner licensing the holder or any other person or corporation, or conveying any rights or permission to manufacture, use, or sell any patented invention that may in any way be related thereto.

50272-101

REPORT DOCUMENTATION PAGE	1. REPORT NO.	2.	3. Recipient's Accession No.

4. Title and Subtitle Moment Method Analysis of the Electric Shielding Factor of a Conducting TM Shield at ELF	5. Report Date April 1995
	6.
7. Author(s) E.H. Newman and M. Kragalott	8. Performing Org. Rept. No. 721566-4
9. Performing Organization Name and Address The Ohio State University ElectroScience Laboratory 1320 Kinnear Road Columbus, OH 43212	10. Project/Task/Work Unit No. 11. Contract(C) or Grant(G) No. (C) N00014-89-J-1007 P00008 (G)
12. Sponsoring Organization Name and Address Department of the Navy, Office of Naval Research 800 N. Quincy St. Arlington, VA 22217-5000	13. Report Type/Period Covered Technical Report 14.

15. Supplementary Notes

16. Abstract (Limit: 200 words)

This report presents an integral equation and method of moments (MM) solution to the problem of TM transmission by a metallic conducting shield at extremely low frequencies (ELF). In order to obtain an accurate and efficient solution the equivalent volume polarization currents representing the shield are expanded in terms of a physical basis expansion corresponding to two plane waves propagating normal to the surface of the shield. ELF approximations are used to obtain closed form expressions for certain crucial elements in the MM matrix equation where extreme accuracy between the *relative* magnitudes of self and mutual impedance terms are required. Numerical data will illustrate that, despite the fact that the equivalent polarization currents are being very accurately computed, the method is not capable of computing the extreme near zone electric and magnetic fields of these currents with sufficient accuracy to compute either the electric or the magnetic shielding factor. An alternate method for computing the shielding factors, based upon the use of the volume equivalence theorem to directly compute the total fields in the shield is devised. This alternate method is found to be sufficiently accurate to compute the electric, but not the magnetic shielding factor.

17. Document Analysis a. Descriptors

ABSORBERS
SHIELDING
MOMENT METHOD
2-D

b. Identifiers/Open-Ended Terms

c. COSATI Field/Group

18. Availability Statement	19. Security Class (This Report)	21. No. of Pages
A. Approved for public release; Distribution is unlimited.	Unclassified	38
	20. Security Class (This Page) Unclassified	22. Price

(See ANSI-Z39.18) *See Instructions on Reverse* OPTIONAL FORM 272 (4-77)
Department of Commerce

Contents

List of Figures

Chapter 1

Introduction

Electromagnetic shields are used to reduce the electromagnetic field strengths in a volume of space due to sources external to that volume. Shields have traditionally been used to reduce electromagnetic interference to sensitive electrical equipment. More recently there is a growing concern over the potential harmful biological effects of the electromagnetic fields radiated by 60 Hz power lines [1], and this report focuses on the extremely low frequency (ELF) shielding problem. The problem of electromagnetic shielding has been considered by a number of authors [2]-[10], however, except for recent work involving the finite element method [11] this work has been primarily limited to shields of simple shape such as planar, circular cylindrical, and spherical. Here we present an integral equation and method of moments (MM) [12] solution for TM to z ELF transmission by a conducting cylindrical shield of essentially arbitrary shape.

The basic theory for the integral equation and MM solution for the TM shield is identical to that for the TM dielectric cylinder and is thus well known [12, Sec. 3-7],[14] and has been implemented in terms of user oriented computer codes [15]. However, it is felt that these standard methods and codes will fail when applied to the problem of the ELF shield. The reason is that while the shields are always extremely thin in terms of a free space wavelength, they are typically comparable to a wavelength in the shield medium. For example, for an aluminum shield of conductivity $\sigma = 35\text{M}\mho/\text{m}$, and thickness $T = 1\text{cm}$ at a frequency of $f = 60\text{Hz}$,

$$k_0 T = 1.26 \times 10^{-8} \quad \text{and} \quad \gamma T = 0.911 + j0.911$$

where k_0 is the free space wavenumber and γ is the propagation constant in the shield medium. Virtually all MM codes applicable to arbitrary geometries employ subsectional basis functions [12, Sec. 1.5]. In general it will be necessary to have several subsectional basis functions per $|\gamma|T$ to model the variation of the fields through the thickness of the shield. It has been found that the accuracy of the MM solution is critically dependent upon the accurate computation of the self and mutual impedances between these basis functions. However, few codes are written to accurately distinguish between the self impedance of a basis function and a mutual impedance when the separation is on the order of $k_0 T = 10^{-8}$.

Section 2 presents the basic theory for the volume integral equation and its solution by the MM. In order to have an efficient solution, which avoids the need for several subsectional basis functions per $|\gamma|T$ through the thickness of the shield, a physical basis [16] expansion for the current is employed. This physical basis expansion represents the volume equivalent shield current in terms of an Outer mode corresponding to fields propagating from the outer to the inner surface of the shield, and an Inner mode corresponding to fields propagating from the inner to the outer surface of the shield. When presenting expressions for the elements in the MM matrix equation, emphasis is placed upon the use of ELF approximations to obtain closed form expressions which insure the proper *relative* magnitude for the self and mutual impedances between the Outer and Inner modes. In Section 3, numerical results are shown to illustrate the accuracy and limitations of the method. In brief, it is found that the MM solution can accurately compute the equivalent current representing the shield. However, the current is not sufficiently accurate to compute the extreme near zone fields, and thus is not sufficiently accurate to directly compute either the electric or the magnetic shielding factors. An alternate method for computing the shielding factors is presented which yields good results for the electric but not the magnetic shielding factor.

Chapter 2

Theory

2.1 The Volume Integral Equation

Figure 2.1(a) shows the original problem in which the TM to z plane wave

$$\mathbf{E}^i = \hat{\mathbf{z}} E_0 e^{jk_0(x\cos\phi_i + y\sin\phi_i)} \tag{2.1}$$

incident from the angle ϕ_i with respect to the x axis, produces the unknown total electric field, $\mathbf{E}$, when incident on a 2D non-magnetic conducting shield of thickness T. The ambient medium is free space (or any homogeneous medium) with material parameters (μ_0, ϵ_0), intrinsic impedance $\eta_0 = \sqrt{\mu_0/\epsilon_0}$, and wavenumber $k_0 = \omega\sqrt{\mu_0\epsilon_0}$, where $\omega = 2\pi f$ is the radian frequency. The inhomogeneous shield Region R, has relative permittivity $\epsilon_r(l)$, conductivity $\sigma(l)$, and complex permittivity

$$\epsilon(l) = \epsilon_r(l)\epsilon_0 - j\frac{\sigma(l)}{\omega} \qquad -\frac{T}{2} \le t \le \frac{T}{2} \tag{2.2}$$

where l measures position along the centerline of the shield. All fields and currents are time harmonic, with the $\exp(j\omega t)$ time dependence suppressed.

As illustrated in Figure 2.1(b), the first step in obtaining the integral equation is to use the volume equivalence theorem [17, Sec. 3-11], [18, Sec. 7.7] to replace the shield by free space and by the unknown equivalent electric volume polarization currents

$$\mathbf{J} = j\omega(\epsilon - \epsilon_0)\mathbf{E} \quad \text{in } R. \tag{2.3}$$

In the equivalent problem of Figure 2.1(b), the total electric field, $\mathbf{E}$ at any point in space, is the superposition of the incident electric field of Equation (2.1) plus the free

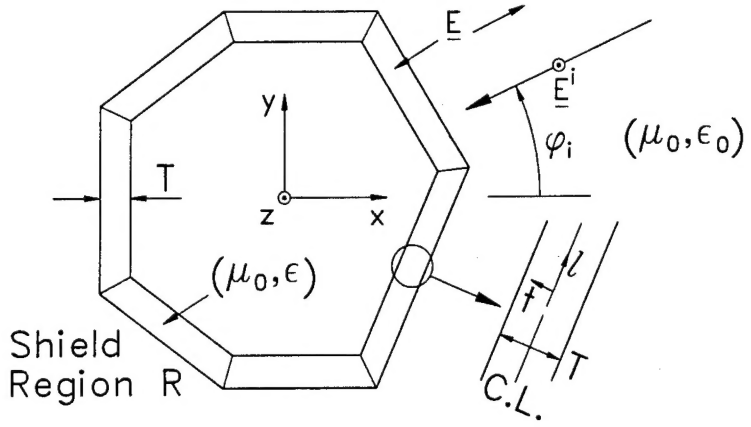

(a) The Original Problem

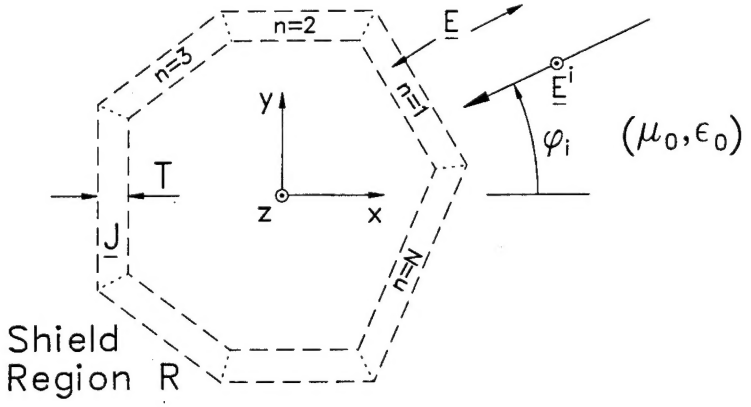

(b) The Equivalent Problem

Figure 2.1: (a) A TM polarized plane wave is incident upon a conducting shield; (b) the shield is replaced by free and the equivalence volume polarization current **J**.

space fields of $\mathbf{J}$, i.e.,

$$\mathbf{E} = \mathbf{E}^i + \mathbf{E}^{\mathbf{J}} \qquad \text{all space} \tag{2.4}$$

where $\mathbf{E}^{\mathbf{J}}$ is the free space electric field of $\mathbf{J}$. For the TM polarization, all electric fields and equivalent electric currents are $\hat{\mathbf{z}}$ directed, and thus the vector notation will be dropped. Inserting Equation (2.4) into (2.3) results in the volume integral equation [14], [12, Sec. 3-7]

$$-E^J + \frac{J}{j\omega(\epsilon - \epsilon_0)} = E^i \qquad \text{in } R. \tag{2.5}$$

2.2 MM Solution

The first step in the MM [12] solution of Equation (2.5) is to expand the unknown current $J(l,t)$ in terms of an appropriate set of expansion functions. Although the actual shield may be curved, as illustrated in Figure 2.1, for the purpose of defining the expansion functions the cross section region of the shield is approximated by N thin trapezoidal cells. Let ϵ_n denote the assumed constant value of ϵ in cell n. E and J will be approximated as being independent of l within each trapezoidal cell. By contrast, E and J should not be approximated as constant through the thickness ($-T/2 \leq t \leq T/2$) of the shield, since typically T will be on the order of a few skin depths, δ, in the shield material. As illustrated in Figure 2.2(a), if a standard subsectional expansion (such as pulse or triangular) is used for the t variation of $J(l,t)$, then several subsections per skin depth would be required through the shield thickness. Assuming that 10 subsections per δ are required, the total number of subsections or unknowns would be $10NT/\delta$ which would become large if $T \gg \delta$.

To avoid the necessity of several unknowns per T/δ inherent in a standard subsectional expansion, we will employ a *physical basis* expansion [13]. The physical basis expansion is based upon the physical insight that when an electromagnetic wave in free space hits the interface of a medium of much higher density, the wave which is transmitted into the higher density medium will propagate almost normal to the interface. In our case, the shield medium is typically a good conductor (with σ on the order of $10^7 \mho/\text{m}$) and is much denser than free space. Thus, there will be a wave with

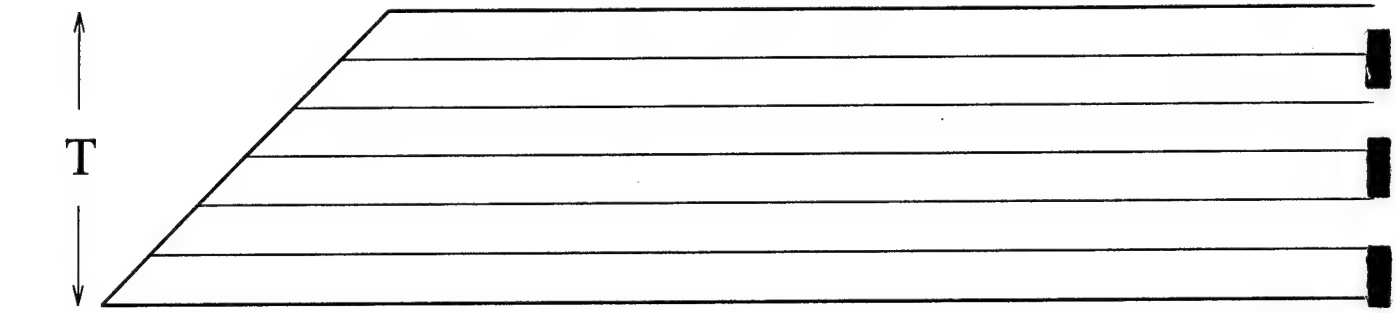

(a) Standard Subsectional Expansion in Cell n

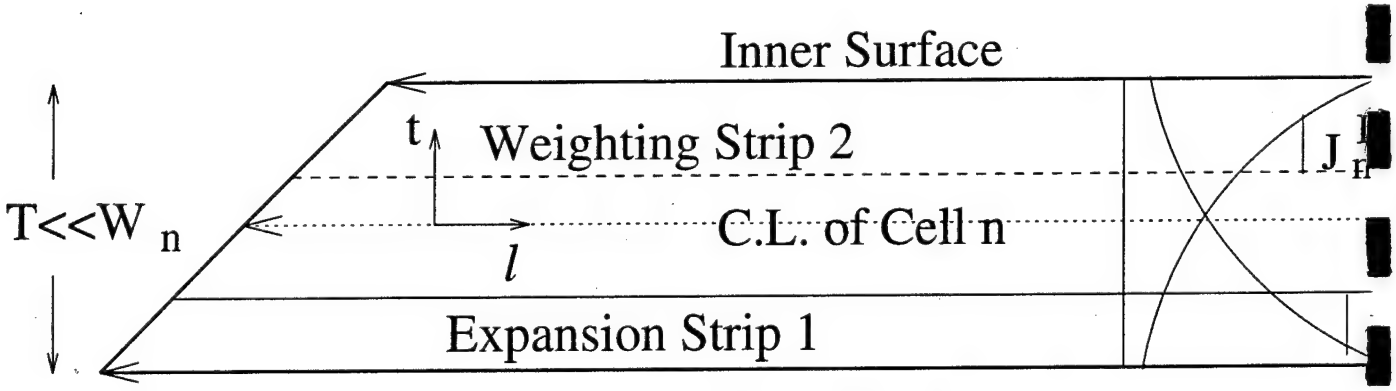

(b) Physical Basis Expansion in Cell n

Figure 2.2: (a) A standard subsectional and (b) physical basis expansion for the current in trapezoidal cell n.

t variation of the form $\exp(-\gamma t)$ propagating from the outer to the inner surface of the shield, where $\gamma = \omega\sqrt{\mu_0\epsilon}$ is the propagation constant in the shield medium. When this wave hits the inner interface at $t = T/2$, it will produce a reflected wave with t variation of the form $\exp(+\gamma t)$. Thus, as illustrated in Figure 2.2(b), the current in the nth trapezoidal cell will be expanded in terms of the Outer and Inner physical basis expansion functions

$$\begin{aligned} J_n^O(t) &= K_n e^{-\gamma_n t} \quad \text{A/m}^2 \text{ in cell } n, \text{ 0 otherwise} \\ J_n^I(t) &= K_n e^{+\gamma_n t} \quad \text{A/m}^2 \text{ in cell } n, \text{ 0 otherwise} \end{aligned} \tag{2.6}$$

where $\gamma_n = w\sqrt{\mu_0\epsilon_n}$ and K_n is a normalizing constant chosen here such that

$$\int_{-T/2}^{T/2} J_n^{O,I}(t)\, dt = 1 \quad \text{A/m} \tag{2.7}$$

and thus

$$K_n = \frac{\gamma_n}{2\sinh(\gamma_n T/2)} \rightarrow \frac{1}{T} \text{ as } |\gamma_n|T \rightarrow 0. \tag{2.8}$$

The physical basis expansion for $J(l,t)$ is

$$J(l,t) \approx \sum_{n=1}^{N} I_n^O J_n^O(t) + I_n^I J_n^I(t) \tag{2.9}$$

in which the I_n^O and I_n^I are N unknown coefficients in the expansions for the Outer and Inner currents, respectively, and involves $2N$ unknowns regardless of T/δ.

Substituting the expansion of Equation (2.9) into the volume integral Equation (2.5) yields

$$-\left[\sum_{n=1}^{N} I_n^O E_n^O + I_n^I E_n^I\right] + \left[\sum_{n=1}^{N} \frac{I_n^O J_n^O(t) + I_n^I J_n^I(t)}{jw(\epsilon_n - \epsilon_0)}\right] = E^i \quad \text{in } R \tag{2.10}$$

where $E_n^{O,I}$ is the free space electric field of expansion function $J_n^{O,I}$. Employing Galerkin's method, with weighting functions chosen identical to the expansion functions, we multiply both sides of Equation (2.10) by J_m^O $(m = 1, 2, \ldots, N)$ and integrate over the cross section Region R of the shield. Next, we multiply both sides of Equation (2.10) by J_m^I $(m = 1, 2, \ldots, N)$ and again integrate over the cross section Region R of the shield. This will reduce Equation (2.10) to an order $2N$ matrix equation

which can be written in block matrix form as

$$\begin{bmatrix} Z^{OO} + \Delta Z^{OO} & Z^{OI} + \Delta Z^{OI} \\ Z^{IO} + \Delta Z^{IO} & Z^{II} + \Delta Z^{II} \end{bmatrix} \begin{matrix} I^O \\ I^I \end{matrix} = \begin{matrix} V^O \\ V^I \end{matrix} \tag{2.11}$$

in which the first superscript indicates the weighting function and the second the expansion function, and I^O and I^I are length N vectors which hold the I_n^O and I_n^I coefficients from the expansion of Equation (2.9). Typical elements of the symmetric MM matrix equation are for $m, n = 1, 2, \ldots, N$

$$Z_{mn}^{PQ} = -\int_m E_n^Q J_m^P \, ds = Z_{nm}^{QP} \tag{2.12}$$

$$\Delta Z_{mn}^{PQ} = \int_m \frac{J_n^Q J_m^P}{j\omega(\epsilon_n - \epsilon_0)} \, ds = \Delta Z_{nm}^{QP} \tag{2.13}$$

$$V_m^P = \int_m E^i J_m^P \, ds \tag{2.14}$$

in which expansion function P and weighting function Q are O or I for the Outer or Inner basis functions, respectively, and where the integrals are over the cross section region of trapezoidal weighting cell m. The $[\Delta Z]$ matrices are diagonal since their integrands are non zero only when $m = n$. If trapezoidal cell n is approximated as a rectangular cell of width W_n and thickness T, then the diagonal $[\Delta Z]$ matrices reduce to

$$\Delta Z_{nn}^{OO} = \Delta Z_{nn}^{II} = \frac{W_n K_n^2}{j\omega(\epsilon_n - \epsilon_0)\gamma_n} \sinh \gamma_n T \tag{2.15}$$

$$\Delta Z_{nn}^{OI} = \Delta Z_{nn}^{IO} = \frac{W_n K_n^2}{j\omega(\epsilon_n - \epsilon_0)} T. \tag{2.16}$$

2.3 Same Cell Impedance Terms

The solution of the MM matrix Equation (2.11) is critically dependent upon the difference between the self impedance of the Outer or Inner basis functions and the mutual impedance between the Outer and Inner basis functions in the same cell, i.e., on

$$Z_{nn}^{OO} - Z_{nn}^{OI} \quad \text{or} \quad Z_{nn}^{II} - Z_{nn}^{IO}. \tag{2.17}$$

At ELF these impedance differences are extremely small, and special care must be taken so that the subtractions in Equations (2.17) are accurate. To accomplish this,

we obtain closed form expressions for these impedances written as the sum of a large term, which is identical for all four impedances, plus small terms.

Figure 2.2(b) shows trapezoidal cell n of inner width W_n^I, outer width W_n^O, and center width W_n. Letting P or Q be O or I, the four self and mutual impedances in cell n can be written as

$$Z_{nn}^{PQ} = \int_{-T/2}^{T/2} \int_{-T/2}^{T/2} Z_{21}(t,t') J_n^P(t) J_n^Q(t')\, dt\, dt' \qquad P,Q = O,I \tag{2.18}$$

in which $Z_{21}(t,t')$ is the mutual impedance between expansion Strip 1 at t' and weighting Strip 2 at t. Appendix A uses ELF approximations to develop simple expressions for this mutual impedance as a function of the strip widths and separations. The width of Strips 1 and 2 can be written as

$$W_1(t') = W_n + \alpha_n t' \text{ and } W_2(t) = W_n + \alpha_n t \tag{2.19}$$

in which $\alpha_n = (W_n^I - W_n^O)/T$. Inserting Equation (2.19) into either Equation (A.17) or (A.18) and dropping second order small terms yields

$$\begin{aligned} Z_{21}(t,t') &= Z_{12}(t',t) \approx Z_{nn} - C\alpha_n W_n (t+t') \\ &+ j\frac{2C}{\pi}\left[\pi W_n |t-t'| + \alpha_n W_n (\ln(bW_n) - 1)(t+t')\right] \end{aligned} \tag{2.20}$$

in which the constants $b = 0.8905 k_0$ and $C = -k_0\eta_0/4$, and Z_{nn} is the self impedance of a strip of width W_n as given by Equation (A.14). Equation (2.20) can be viewed as the first two terms in a Taylor series approximation to $Z_{21}(t,t')$.

Equation (2.20) can be inserted into (2.18) and the integrations can be carried out in closed form. The result is

$$\begin{aligned} Z_{nn}^{PQ} &\approx Z_{nn} - C\alpha_n W_n [I_1(\gamma_P) + I_1(\gamma_Q)] \\ &+ j\frac{2C}{\pi}\left[\pi W_n S(\gamma_P,\gamma_Q) + \alpha_n W_n (\ln(bW_n) - 1)[I_1(\gamma_P) + I_1(\gamma_Q)]\right] \end{aligned} \tag{2.21}$$

in which

$$\begin{aligned} I_1(\gamma_P) &= \int_{-T/2}^{T/2} \int_{-T/2}^{T/2} t J_n^P(t) J_n^Q(t')\, dt'\, dt \\ &= \frac{1}{\gamma_P}\left[\frac{\gamma_P T}{2} \coth \frac{\gamma_P T}{2} - 1\right] \end{aligned} \tag{2.22}$$

$$S(\gamma_P, \gamma_Q) = \int_{-T/2}^{T/2} \int_{-T/2}^{T/2} |t - t'| J_n^P(t) J_n^Q(t')\, dt'\, dt \tag{2.23}$$

$$= \frac{4K_n^2}{\gamma_P^2(\gamma_P + \gamma_Q)} \sinh(\gamma_P + \gamma_Q)\frac{T}{2} + \frac{2K_n \cosh(\gamma_P T/2)}{\gamma_P}[I_2(\gamma_P) - I_1(\gamma_Q)]$$

$$I_2(\gamma) = \frac{1}{\gamma}\left[\frac{\gamma T}{2}\tanh\frac{\gamma T}{2} - 1\right] \tag{2.24}$$

$$\gamma_{P,Q} = \begin{cases} -\gamma_n & P,Q = O \\ +\gamma_n & P,Q = I \end{cases} . \tag{2.25}$$

Note that Equation (2.21) expresses the four self and mutual impedances in cell n as the sum of a large term, Z_{nn} which is the same for all four impedances, plus small terms. This allows the accurate evaluation of the impedance differences in Equation (2.17), and is crucial in obtaining accurate numerical results. Equation (2.21) obeys the reciprocity relationship $Z_{nn}^{OI} = Z_{nn}^{IO}$, and further these mutual impedances are independent of α_n. However, $Z_{nn}^{OO} \neq Z_{nn}^{II}$ except for rectangular cells with $\alpha_n = 0$.

As a numerical example, Figure 2.3 shows trapezoidal cell n of thickness T, center-line width $W_n = 1$ m, Outer width $W_n^O = W_n + T/2$, Inner width $W_n^I = W_n - T/2$ and conductivity $\sigma = 35\text{M}\mho/\text{m}$. At $f = 100\text{Hz}$, the figure shows the real and imaginary parts of Z_{nn}^{OO} (solid line), Z_{nn}^{OI} (dashed line) and the self impedance of a strip of width W_n (dotted line) as a function of W_n/T (with T variable and W_n fixed). Note that for large W_n/T (as $T \to 0$), Z_{nn}^{OI} = the Outer to Inner mutual impedance approaches Z_{nn}^{OO} = the Outer to Outer self impedance and Z_{nn} = the self impedance of a strip of width W_n.

2.4 Different Cell Impedance Terms

Referring to Figure 2.4 the four mutual impedances between expansion cell n and weighting cell m can be written as

$$Z_{mn}^{PQ} = \int_{-T/2}^{T/2} \int_{-T/2}^{T/2} Z_{21}(t,t') J_m^P(t) J_n^Q(t')\, dt\, dt' \qquad P,Q = O,I \tag{2.26}$$

in which $Z_{21}(t,t')$ is the mutual impedance between expansion Strip 1 at t' in cell n and weighting Strip 2 at t in cell m. Closed form expressions for $Z_{21}(t,t')$ are given in Appendix B. The remaining double integral in Equation (2.26) is done numerically.

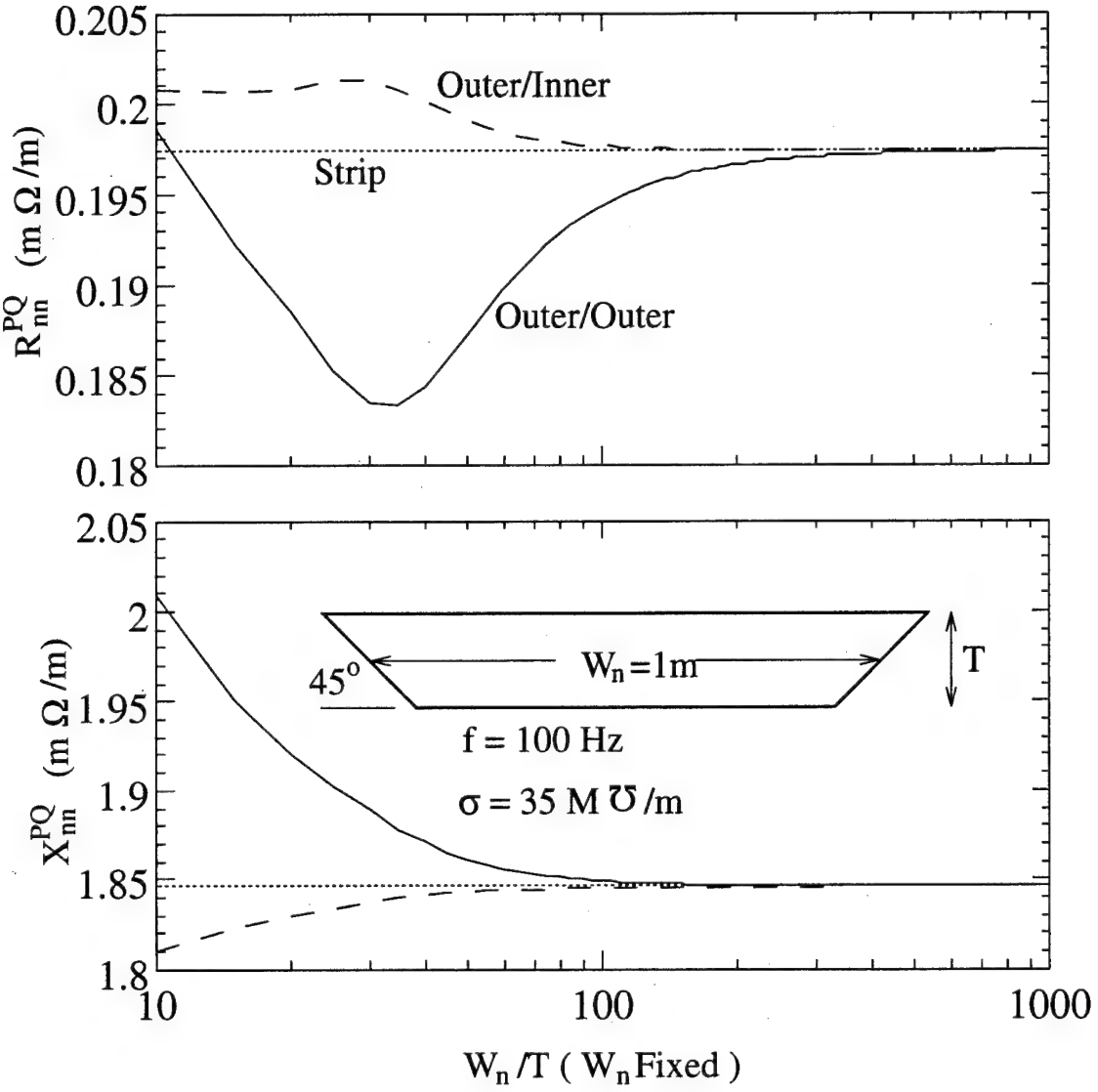

Figure 2.3: The self and mutual impedances between the Outer and Inner modes in a trapezoidal cell as a function of the thickness T.

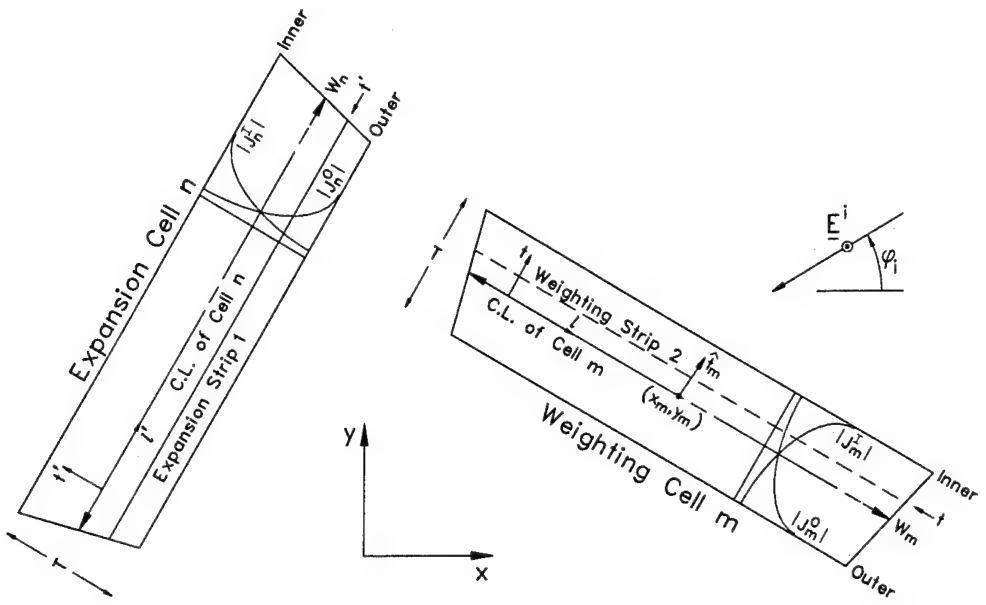

Figure 2.4: The reaction between the Inner and Outer modes in weighting cell m and the incident plane wave.

2.5 The Voltage Vector

Referring to Figure 2.4, a typical element of the voltage vector, Equation (2.14), can be written as

$$V_m^P = \int_{-T/2}^{T/2} V_m(t) J_m^P(t)\, dt \tag{2.27}$$

where $V_m(t)$ is the reaction between the incident field of Equation (2.1) and a unit amplitude strip at position t in cell m. The reaction between this incident field and a unit amplitude strip of width W centered at (x, y) and making an angle ψ with respect to the $+x$ axis, is

$$V(x,y) = E_0 e^{j\Phi(x,y)} \frac{2\sin[0.5k_0 W\cos(\psi-\phi_i)]}{k_0\cos(\psi-\phi_i)} \tag{2.28}$$

in which

$$\Phi(x,y) = k_0(x\cos\phi_i + y\sin\phi_i) \tag{2.29}$$

is the phase of the incident plane wave of Equation (2.1) at the center of the strip. At ELF, $k_0 W \ll 1$, and Equation (2.28) reduces to

$$V(x,y) \approx E_0 W(1 + j\Phi(x,y)). \tag{2.30}$$

The (x, y) coordinates of the center of the strip at position t in Figure 2.4 are

$$x = x_m + t_{mx}t \quad \text{and} \quad y = y_m + t_{my}t \tag{2.31}$$

where $\hat{\mathbf{t}}_m = t_{mx}\hat{\mathbf{x}} + t_{my}\hat{\mathbf{y}}$ is a unit vector in the $+t$ direction in cell m. Then using Equations (2.19) and (2.31) in (2.30), the ELF approximation to the reaction between the incident plane wave and the strip at t is

$$V(t) \approx E_0(W_m + \alpha_m t)\{1 + jk_0[(x_m + t_{mx}t)\cos\phi_i + (y_m + t_{my}t)\sin\phi_i]\}. \tag{2.32}$$

Expanding Equation (2.32) and dropping terms of order t^2 yields

$$V(t) = V_{m0} + jE_0W_m t\Phi(t_{mx}\cos\phi_i, t_{my}\sin\phi_i) + \frac{\alpha_m}{W_m}tV_{m0} \tag{2.33}$$

where $V_{m0} \approx E_0W_m[1 + j\Phi(x_m, y_m)]$ is the reaction between the incident plane wave and the centerline strip in cell m. Inserting Equation (2.33) into (2.27), and using the integral of Equation (2.22), the reaction between the incident plane wave and the Inner or Outer weighting function in cell m is

$$V_m^P = V_{m0} + \left\{\frac{\alpha_m}{W_m}V_{m0} + jE_0W_m\Phi(t_{mx}\cos\phi_i, t_{my}\sin\phi_i)\right\} I_1(\gamma_P) \tag{2.34}$$

with γ_P given by $+$ or $-$ γ_m for the Inner or Outer current, respectively. Note that V_m^P is written as the sum of a large term, V_{m0}, plus small terms.

2.6 Shielding Factor

2.6.1 Method 1: Direct Computation

The electric shielding factor is defined by

$$SF_e(x, y) = \frac{|\text{Electric Field at } (x, y) \text{ With the Shield}|}{|\text{Electric Field at } (x, y) \text{ Without the Shield}|} \tag{2.35}$$

$$= \frac{|E^i(x, y) + E^S(x, y)|}{|E^i(x, y)|}. \tag{2.36}$$

E^S is the scattered electric field, i.e., the free space electric field of the equivalent polarization currents of Equation (2.9), and is given by

$$E^S(x, y) = \sum_{n=1}^{N} I_n^O E_n^O(x, y) + I_n^I E_n^I(x, y) \tag{2.37}$$

where $E_n^{O,I}$ is the free space electric field of expansion current $J_n^{O,I}$. $E_n^{O,I}$ can be computed as

$$E_n^{O,I}(x,y) = \int_{-T/2}^{T/2} J_n^{O,I}(t') E_1(t';x,y)\, dt' \tag{2.38}$$

where as given by Equation (A.4), $E_1(t';x,y)$ is the free space electric field of a unit amplitude strip located at position t' in trapezoidal cell n.

In a parallel fashion, one can define the magnetic shielding factor as

$$SF_m(x,y) = \frac{|\text{Magnetic Field at } (x,y) \text{ With the Shield}|}{|\text{Magnetic Field at } (x,y) \text{ Without the Shield}|} \tag{2.39}$$

$$= \frac{|\mathbf{H}^i(x,y) + \mathbf{H}^S(x,y)|}{|\mathbf{H}^i(x,y)|}. \tag{2.40}$$

$\mathbf{H}^S$ is the scattered magnetic field, i.e., the free space magnetic field of the equivalent polarization currents of Equation (2.9) and is given by

$$\mathbf{H}^S(x,y) = \sum_{n=1}^{N} I_n^O \mathbf{H}_n^O(x,y) + I_n^I \mathbf{H}_n^I(x,y) \tag{2.41}$$

where $\mathbf{H}_n^{O,I}$ is the free space magnetic field of expansion current $J_n^{O,I}$. $\mathbf{H}_n^{O,I}$ can be computed as

$$\mathbf{H}_n^{O,I}(x,y) = \int_{-T/2}^{T/2} J_n^{O,I}(t') \mathbf{H}_1(t';x,y)\, dt' \tag{2.42}$$

where as given by Equation (A.7), $\mathbf{H}(t';x,y)$ is the free space magnetic field of a unit amplitude strip located at position t' in trapezoidal cell n.

Direct computation of the shielding factors using Equations (2.35)-(2.42) is extremely difficult for two reasons. First, as pointed out by Demarest and Garbacz [19] it is notoriously difficult to accurately compute extreme near zone fields with the MM. In particular, small variations in the current and its derivatives, caused by such factors as the choice of expansion and weighting functions, can result in large variations of the extreme near zone fields. Second, as the shielding factors go to zero, the scattered fields must approach the *negative* of the incident fields, and extreme accuracy is required in order to accurately compute (in effect) the subtraction of two nearly equal numbers in the numerators of Equations (2.36) and (2.40). For example, for a shielding factor of 0.01 (-40 dB), the near zone scattered fields would need to be computed to at least three digits of accuracy.

Figure 2.5 illustrates the difficulty in computing the shielding factors using Equations (2.36) and (2.40). The insert in Figure 2.5 shows a perfectly conducting square shield of side length 1 m. The figure shows the electric and magnetic shielding factors at $(x, y) = (0.25, 0.25)$ m, computed by Equations (2.36) and (2.40), respectively, as a function of $N/4$ = the number of pulse expansion functions per side. Since the shield is perfectly conducting, the shielding factors are zero ($-\infty$ dB), and thus this figure shows a lower limit the smallest shielding factors which can be computed via Equations (2.36) and (2.40). As $N/4$ goes from 1 to 19 segments per side, SF_e goes from about -60 to -105 dB. Thus, it may be possible to compute SF_e with Equation (2.36), especially if one is willing to use several segments per side. By contrast, as $N/4$ goes from 1 to 19 segments per side, SF_m goes from about +60 to +20 dB, indicating a complete failure of the MM solution to accurately compute the near zone scattered magnetic field, and thus SF_m via Equation (2.40). Figure 2.6 shows the magnitude of the surface current on the side at $x = 0.5$ m for $N/4 = 1$, 5, and 19 segments per side. As more segments are added, the current shape changes, and attempts to satisfy the edge condition (for a 90° wedge) that the current near the edge approaches infinity as $1/(\text{distance})^{1/3}$ to the edge [20]. It is felt that in order to accurately compute the near zone scattered fields, it would (at a minimum) be necessary to employ MM expansion functions which satisfy the edge condition. While this could be done for the perfectly conducting case [21]-[23], it would be considerably more difficult for finitely conducting shields since the edge condition is not known.

2.6.2 Method 2: Using the Volume Equivalence Theorem

A method for computing the total fields and the shielding factors, without the need to explicitly compute the scattered fields, will now be discussed. Assuming that the MM solution can provide a reasonable approximation to the polarization current, J, then using the volume equivalence theorem of Equation (2.3), it can also provide a reasonable approximation to the *total* electric field in the shield. Substituting Equation (2.9) into (2.3), the ($\hat{\mathbf{z}}$ polarized) electric field in the shield ($-T/2 \leq t \leq T$)

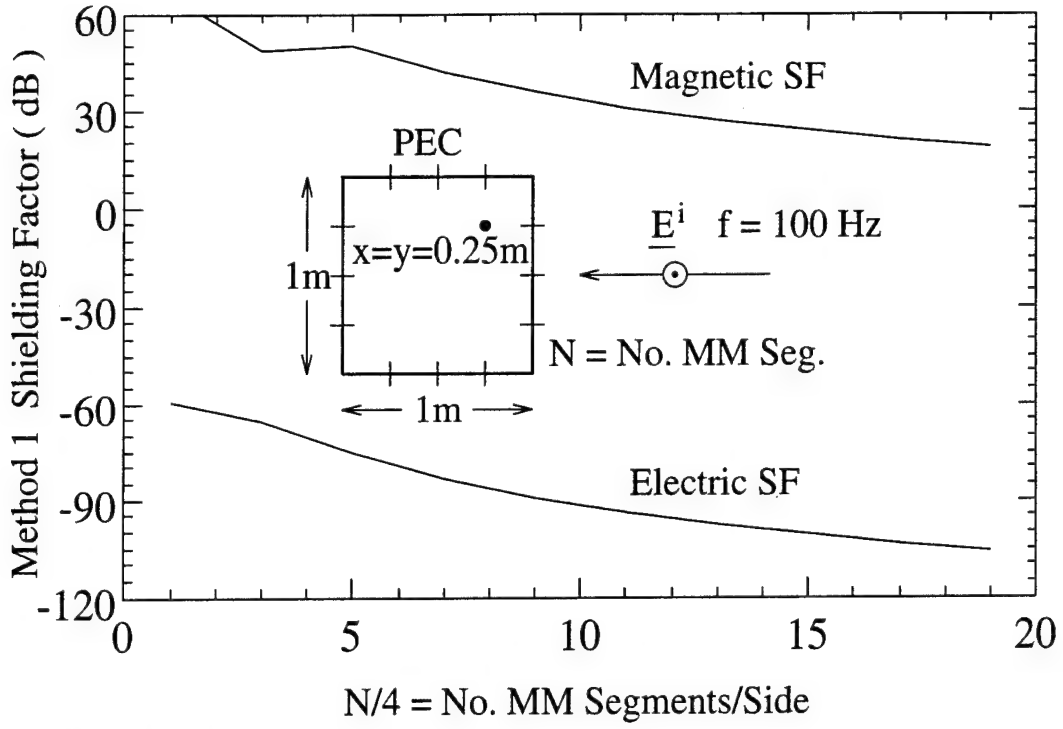

Figure 2.5: The Method 1 electric and magnetic shielding factor for a perfectly conducting square shield as a function of the number of pulse expansion function per side.

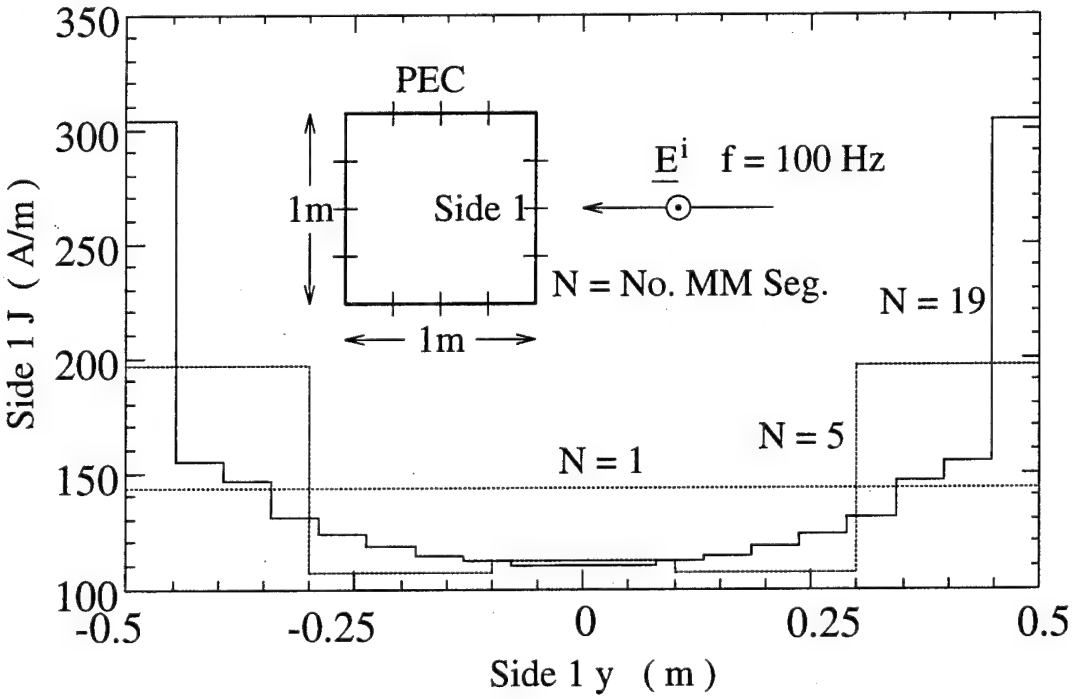

Figure 2.6: The magnitude of the current on Side 1 of a perfectly conducting square shield for $N/4 = 1$, 5, and 19 MM expansion function per side.

is

$$\mathbf{E}(l,t) = \hat{\mathbf{z}}\frac{J(l,t)}{j\omega(\epsilon-\epsilon_0)} \approx \hat{\mathbf{z}}\sum_{n=1}^{N}\frac{I_n^O J_n^O(t) + I_n^I J_n^I(t)}{j\omega(\epsilon_n-\epsilon_0)}. \tag{2.43}$$

Using Equation (2.43) and Maxwell's equations, the magnetic field in the shield is

$$\mathbf{H} = \frac{-1}{j\omega\mu_0}\nabla\times\mathbf{E} = \frac{-1}{j\omega\mu_0}(-\hat{\mathbf{z}}\times\hat{\mathbf{t}})\frac{\partial E}{\partial t} \approx \hat{\mathbf{l}}\sum_{n=1}^{N}\gamma_n\frac{I_n^O J_n^O(t) - I_n^I J_n^I(t)}{\omega^2\mu_0(\epsilon_n-\epsilon_0)} \tag{2.44}$$

where the unit vector $\hat{\mathbf{l}} = \hat{\mathbf{z}}\times\hat{\mathbf{t}}$ is directed parallel to the surface of the shield. The use of Equations (2.43) and (2.44) to compute the near zone fields has two advantages. First, it avoids the anomalous behavior [19] associated with the computation of the extreme near zone scattered fields. Second, it is a direct computation of the *total* electric and magnetic fields, and thus avoids the numerically difficult subtraction of fields in the numerators of Equations (2.36) and (2.40). One difficulty with Equations (2.43) and (2.44) is that they provide the fields in the shield, and not interior to the shield. However, since the tangential electric and magnetic fields are continuous at the interior shield interface, here we simply take the average value of $E_z(l,t=T/2)$ or $H_l(l,t=T/2)$ as representative of the electric or magnetic fields in the interior of the shield, and thus

$$SF_e = \frac{\text{Average } |E_z(l,t=T/2)|}{|E^i(0,0)|} \tag{2.45}$$

$$SF_m = \frac{\text{Average } |H_l(l,t=T/2)|}{|\mathbf{H}^i(0,0)|}. \tag{2.46}$$

In practice, at ELF the fields are almost independent of circumferential position, l, and the average fields can be replaced by the fields at any convenient value of l.

Chapter 3

Numerical Results

The first set of data will illustrate the accuracy and limitations of the MM solution. The insert in Figure 3.1 show an octagonal shield of mean radius 1 m, thickness $T =$ 1 cm, and conductivity $\sigma = 35$ MŬ/m illuminated by a unit amplitude plane wave at $f = 100$ Hz. The MM solution for this octagonal shield will be compared to the eigenfunction solution [13] for a circular shield of the same thickness and conductivity and of mean radius 0.974 m (same circumference as octagon). The figure compares the Equation (2.43) MM (solid line) and eigenfunction computation (dotted line) for the magnitude and phase of the total electric field along a line from the outer surface of the shield ($t/T = -0.5$) to the inner surface of the shield ($t/T = 0.5$). Since from Equation (2.3) the electric field in the shield and the volume polarization current differ by only a scale factor of $j\omega(\epsilon - \epsilon_0)$, Figure 3.1 shows that the MM solution is capable of very accurately computing the t variation of the equivalent current representing the shield. For the same geometry as was considered in Figure 3.1, Figures 3.2(a) and (b) show the Equation (2.44) MM and eigenfunction computation of the magnitude and phase of the magnetic field in the shield. This figure shows that overall the MM is doing a good job of computing the magnetic field in the shield, except very near the inner surface ($t/T = 0.5$). Figure 3.2(c) shows the MM and eigenfunction computation of the magnitude of the magnetic field for the region within 1% of the inner surface, i.e., $0.49 \leq t/T \leq 0.5$, where it can be seen that the eigenfunction magnetic field is much smaller than the MM magnetic field at the inner surface of the shield. For the same geometry as was considered in Figures 3.1 and 3.2, Figure

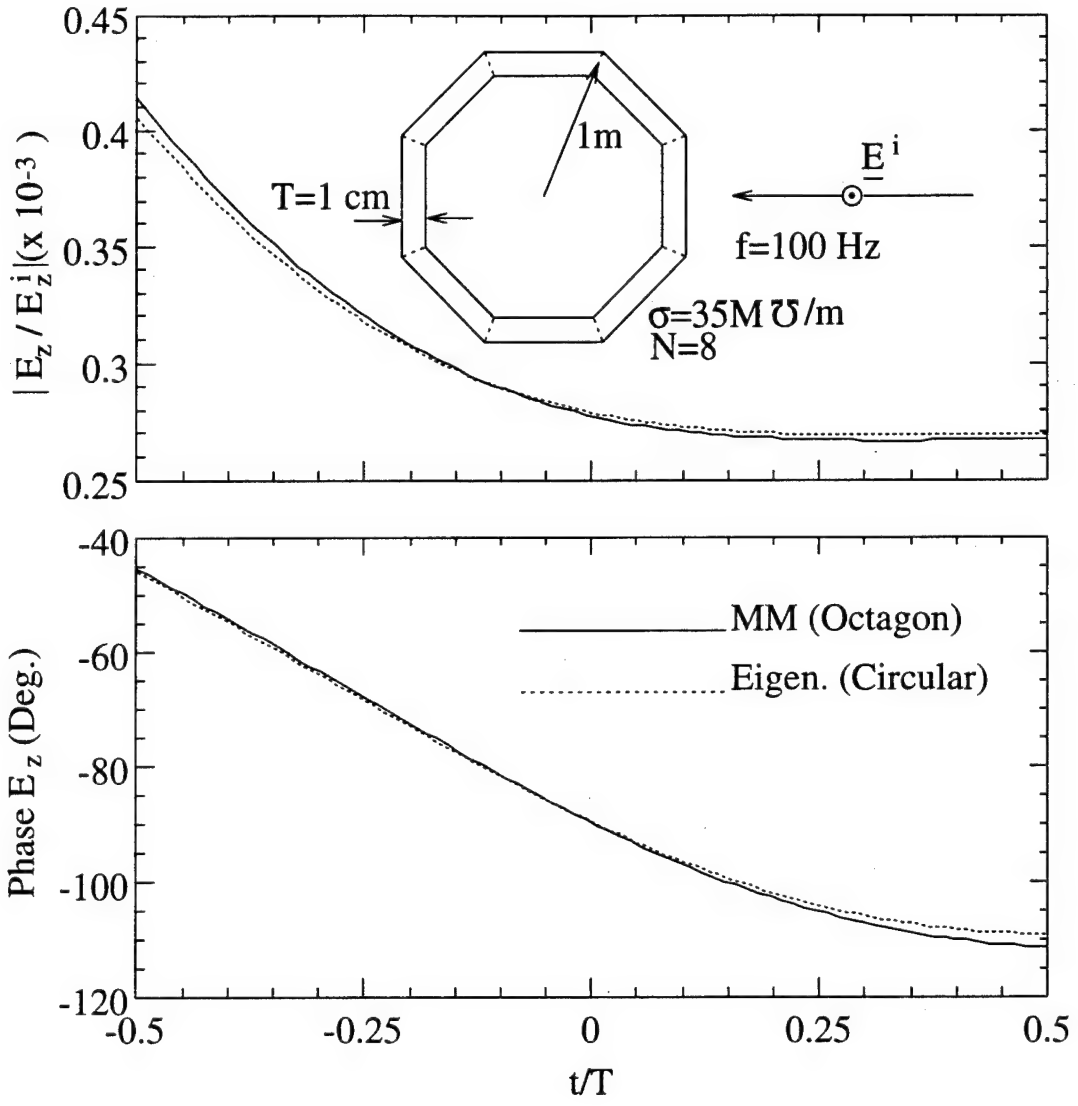

Figure 3.1: The internal electric fields computed by the MM and by an eigenfunction solution.

3.3 shows the ϕ variation of the magnitudes of the electric and magnetic fields along the centerline of the shield, i.e., at $t = 0$. Note that this figure shows only the AC component of the fields computed as the total fields minus the average (over ϕ) fields. Comparing Figures 3.1-3.3 shows that the AC component of the fields are about 4 orders of magnitude smaller than the average fields. Also, the MM solution is doing an excellent job of computing the AC component of the electric field and thus the equivalent polarization currents. By contrast, the AC component of the magnetic fields is only order of magnitude correct.

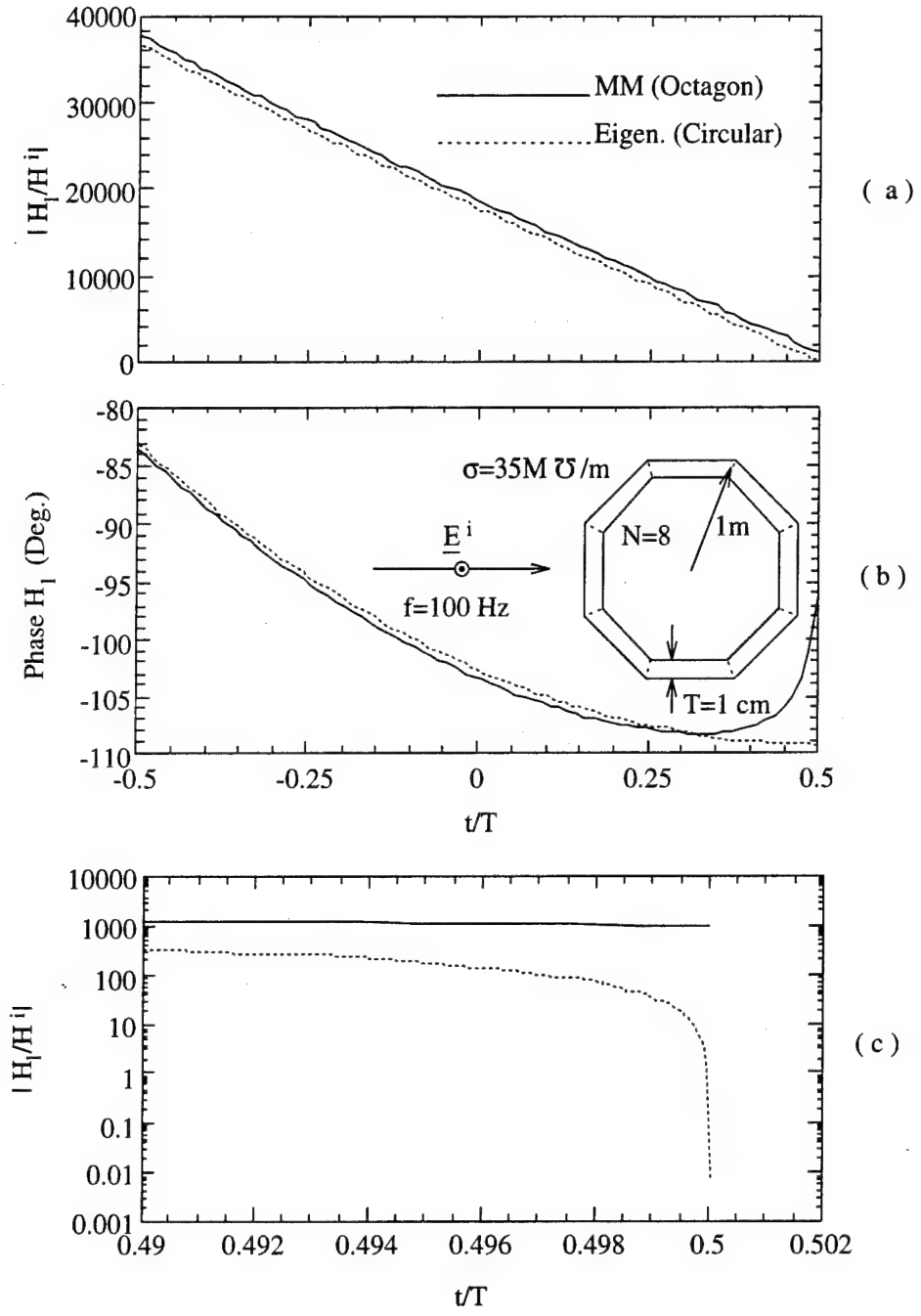

Figure 3.2: The internal magnetic fields computed by the MM and by an eigenfunction solution.

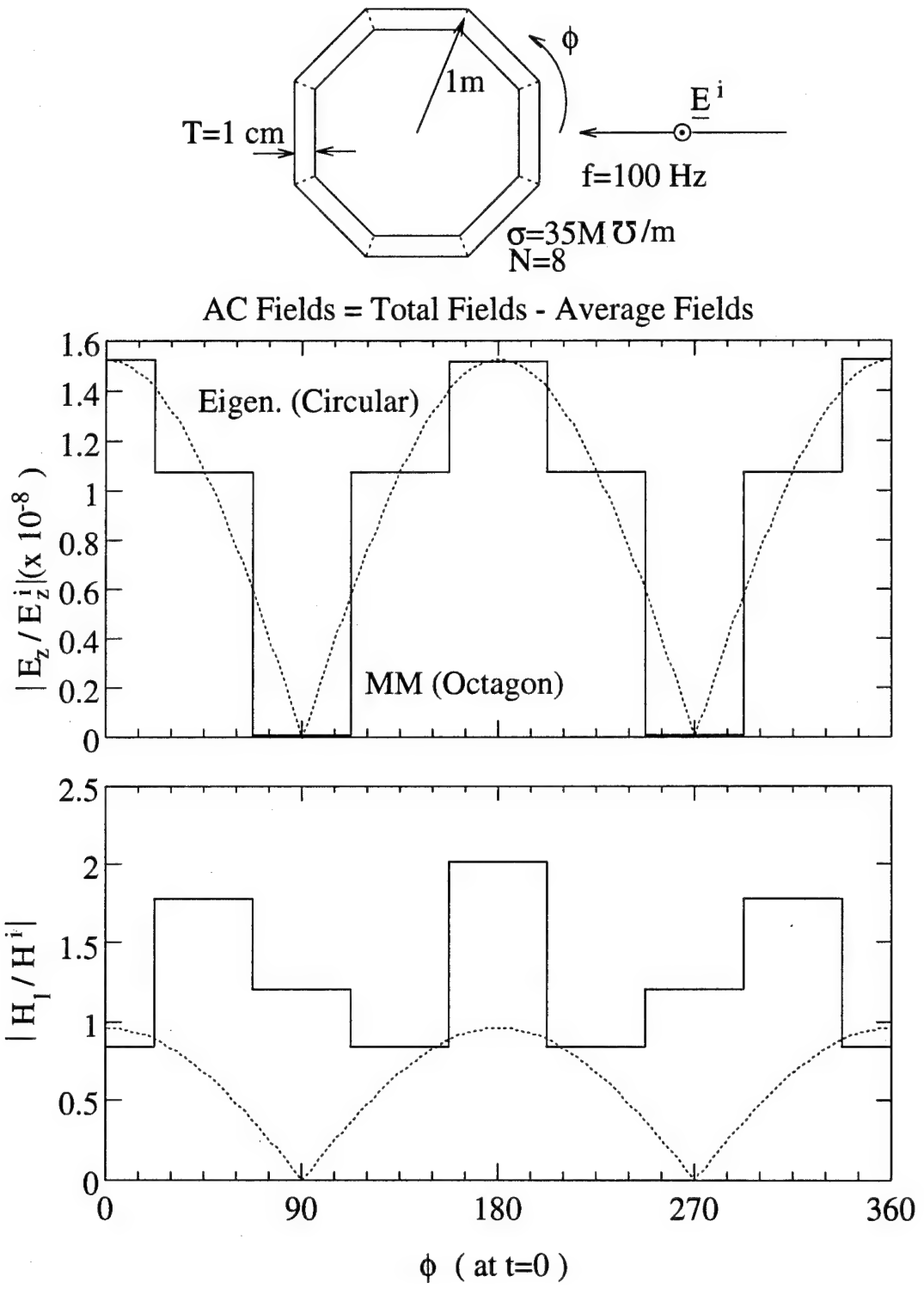

Figure 3.3: The AC component of the internal electric and magnetic fields computed by the MM and by an eigenfunction solution.

Despite the fact that Figures 3.1-3.3 indicate that the MM solution is accurately computing the electric field and thus the equivalent polarization currents representing the shield, these currents are not sufficiently accurate to compute the extreme near zone *scattered* electric or magnetic fields. Thus the MM solution is inadequate to compute the electric or the magnetic shielding factors using the Method 1 Equations (2.36) or (2.40), respectively. By comparison, the Method 2 computation of the shielding factors is dependent upon the computation of the *total* fields at the inner surface $t = T/2$ using Equations (2.43) and (2.44). From Figure 3.1 and 3.2(c), the total fields at the inner surface are

$$\begin{aligned} \text{MM } |E_z(t = 0.5T)| &= 0.000267|E^i| \\ \text{Eigenfunction } |E_z(t = 0.5T)| &= 0.000269|E^i|. \end{aligned} \tag{3.1}$$

$$\begin{aligned} \text{MM } |H_l(t = 0.5T)| &= 975|H^i| \\ \text{Eigenfunction } |H_l(t = 0.5T)| &= 0.00716|H^i|. \end{aligned} \tag{3.2}$$

Thus, the MM solution appears to be more than adequate to compute the electric, but not the magnetic, shielding factor by Method 2. Figure 3.4 compares the MM and eigenfunction solution for the electric shielding factor of an octagonal shield of radius 1m, conductivity $\sigma = 35$ M℧/m and thickness $T = 1$, 0.1, and 0.01cm versus frequency. Note the excellent agreement between the two solutions, and also that by computing SF_e using Method 2 it is possible to compute electric shielding factors as small as -100 dB.

The final set of data will investigate the importance of shield shaping on the electric shielding factor. For example, for a *fixed length* of shielding material, what would be the optimum shape of the shield to minimize SF_e? The insert in Figure 3.5 shows a rectangular shield of height H, width W, thickness $T = 0.1$ cm, and conductivity $\sigma = 35$ M℧/m at $f = 60$ Hz. With the shield perimeter, $2H + 2W$, fixed at 1 m, the figure shows the Method 2 SF_e versus the ratio H/W. Although the worst case or largest SF_e occurs for a square shield with $H = W$, the important point to note from Figure 3.5 is that over a 100:1 range of H/W, SF_e changes by less

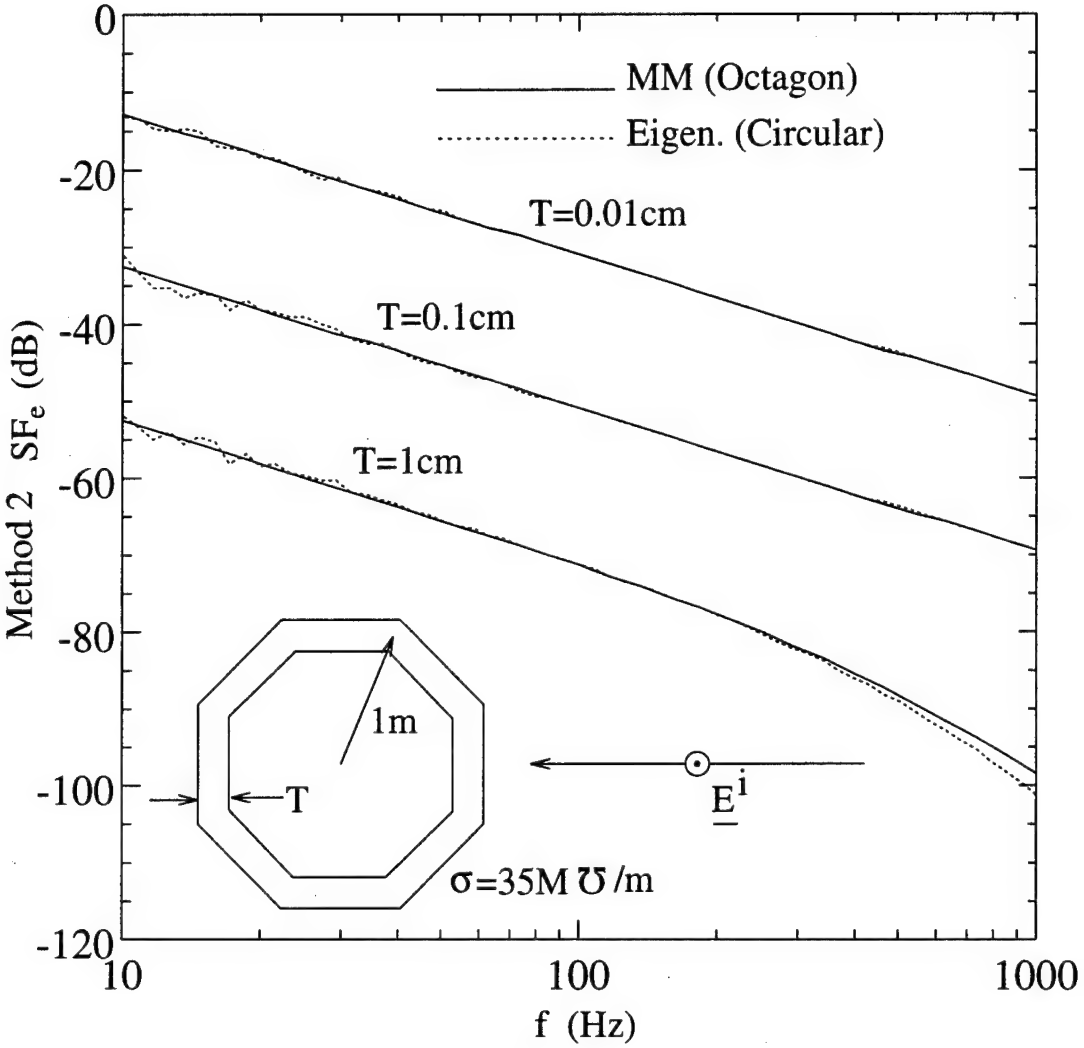

Figure 3.4: The Method 2 electric shielding factor of an octagonal shield versus frequency and computed by the MM and an eigenfunction solution.

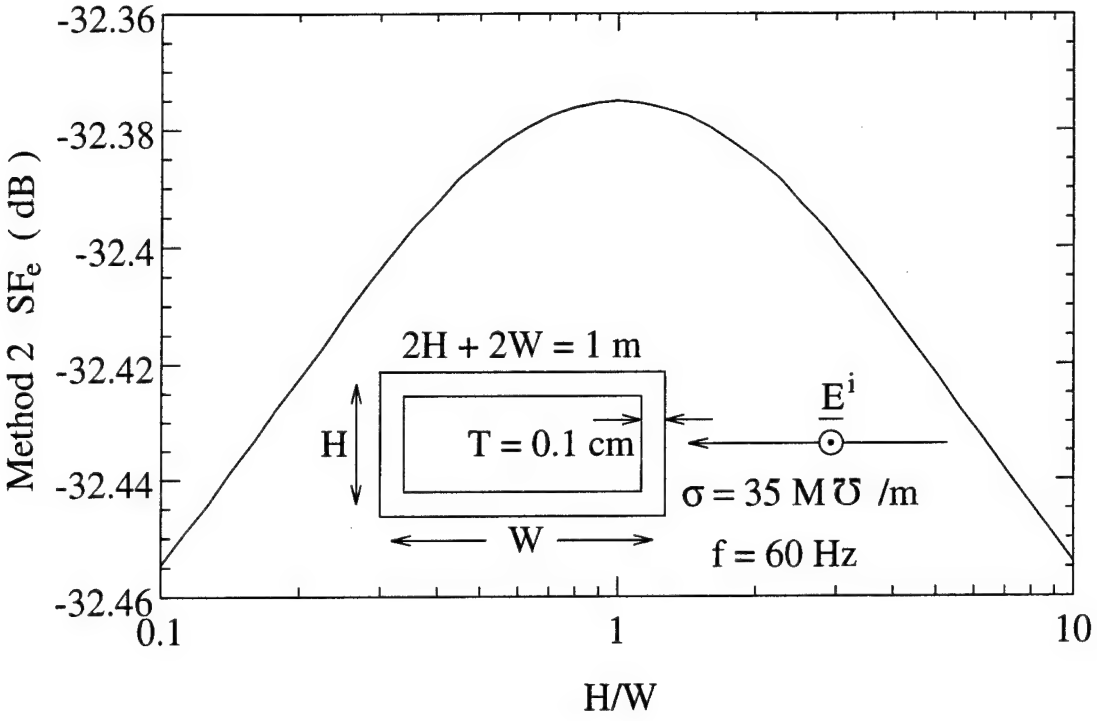

Figure 3.5: The Method 2 electric shielding factor versus the ratio of the height to the width for a rectangular shield of perimeter 1 m.

than 0.1 dB. Thus, for a shield of fixed perimeter, the shape of the shield appears to have little effect on the electric shielding factor. For a square shield of conductivity $\sigma = 35$ MΩ/m at $f = 60$ Hz, Figure 3.6 shows SF_e versus its perimeter for $T = 1$, 0.1, 0.01, and 0.001 cm.

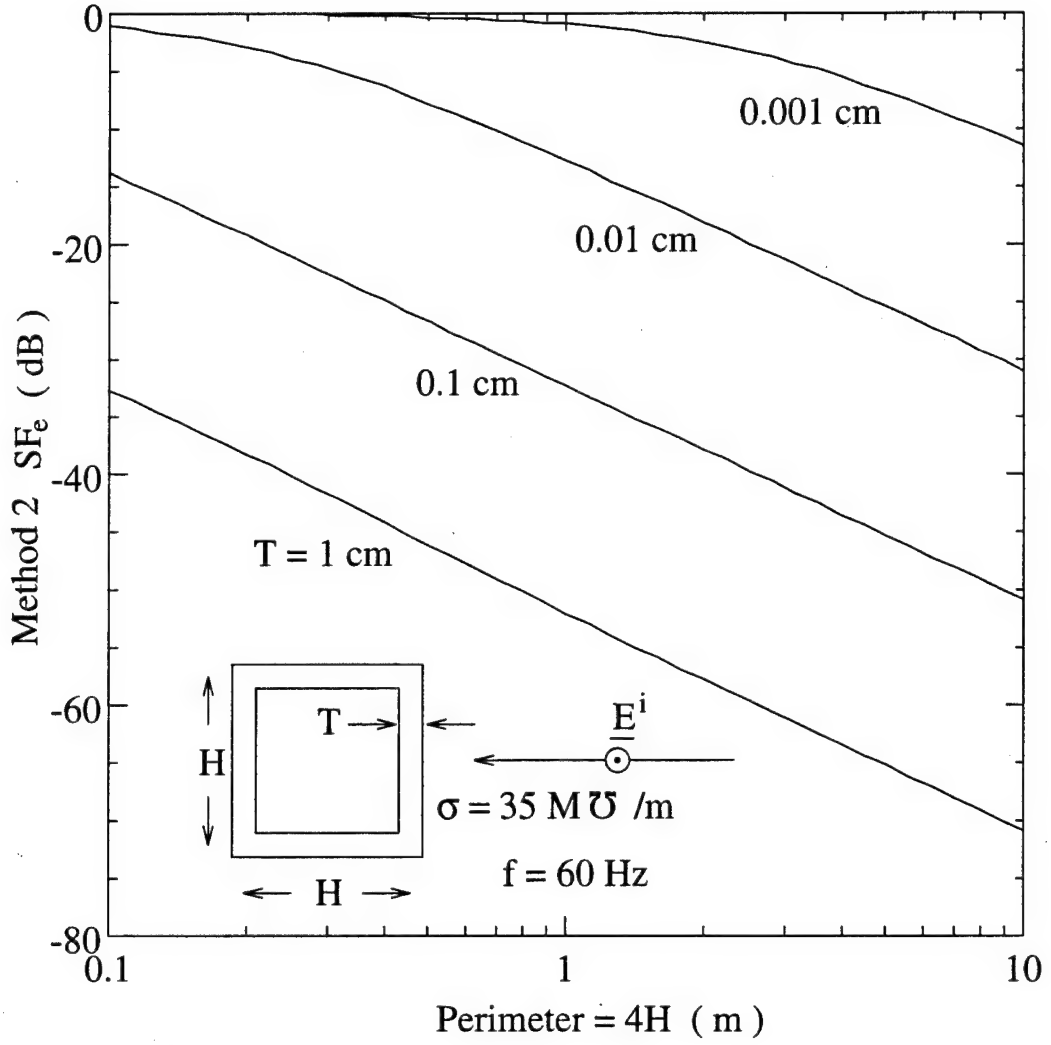

Figure 3.6: The Method 2 electric shielding factor versus the perimeter of an aluminum shield at $f = 60$ Hz.

Chapter 4

Conclusions

This report has presented an integral equation and MM solution to the problem of TM transmission by a conducting shield at ELF. The equivalent volume polarization currents representing the shield are expanded in terms of physical basis functions corresponding to plane waves propagating from the outer to the inner and the inner to the outer surfaces of the shield. The MM solution for an octagonal shield is found to yield a current distribution which is in very close agreement with an eigenfunction solution for a circular shield. However, this current is not sufficiently accurate to compute the extreme near zone fields, and thus is not sufficiently accurate to directly compute the electric or magnetic shielding factors. An alternate method for computing the shielding factors is devised, based upon the use of the volume equivalence theorem to compute the total fields. This alternate method is found to be adequate to compute the electric, but not the magnetic, shielding factor.

One approach to improving the MM solution would be to try to find better expansion and weighting functions and also to more accurate methods for computing the elements in the MM matrix equation. It is the authors judgement that this approach is unlikely to produce the required accuacy. A second approach would be to augment the standard MM matrix equation with additional equations which enforced continuity of the tangential fields at the inner and outer surfaces of the shield. These equations would then be solved on a least squares basis.

Appendix A

Mutual Impedance Between Parallel Strips

This appendix will present approximate closed form expressions for the mutual impedance between parallel strips. Without loss of generality, Figure A.1(b) shows Strip 1 of width W_1 located along the $+y$ axis. Strip 2 is of width W_2 and is translated a distance (x_c, y_c) from the origin. Both strips have unit surface current, i.e., $J_1 = J_2 = 1$ A/m. By definition, the mutual impedance between expansion current J_1 and weighting current J_2 is

$$Z_{21} = -\int_{y_c}^{y_c+W_2} E_1(x_c, y) J_2 \, dy \tag{A.1}$$

where E_1 is the free space electric field of J_1 given by

$$E_1(x, y) = C \int_0^{W_1} J_1 H_0^{(2)}(k_0 \rho') \, dy' \qquad C = -\frac{k_0 \eta_0}{4} \tag{A.2}$$

and where $\rho' = \sqrt{x^2 + (y - y')^2}$ is the distance from the source point $(0, y')$ to the field point (x, y). At ELF, $k_0 \rho' \ll 1$, and the Hankel function in Equation (A.2) can be approximated by [24]

$$H_0^{(2)}(k_0 \rho') \approx 1 - \frac{j2}{\pi} \ln(b\rho') \qquad b = 0.8905 k_0. \tag{A.3}$$

Inserting Equation (A.3) into (A.2) and integrating [25] yields

$$E_1(x, y) \approx C W_1 + j \frac{2C}{\pi} \{[\Delta y_b \ln b\rho_b - \Delta y_b + x\psi_b] - [\Delta y_a \ln b\rho_a - \Delta y_a + x\psi_a]\} \tag{A.4}$$

where as seen in Figure A.1(a), $\Delta y_a = y$ and $\Delta y_b = y - W_1$ are the y coordinates of the field point (x, y) with respect to ends a and b of Strip 1, and

$$\rho_{a,b} = \sqrt{x^2 + \Delta y_{a,b}^2} \tag{A.5}$$

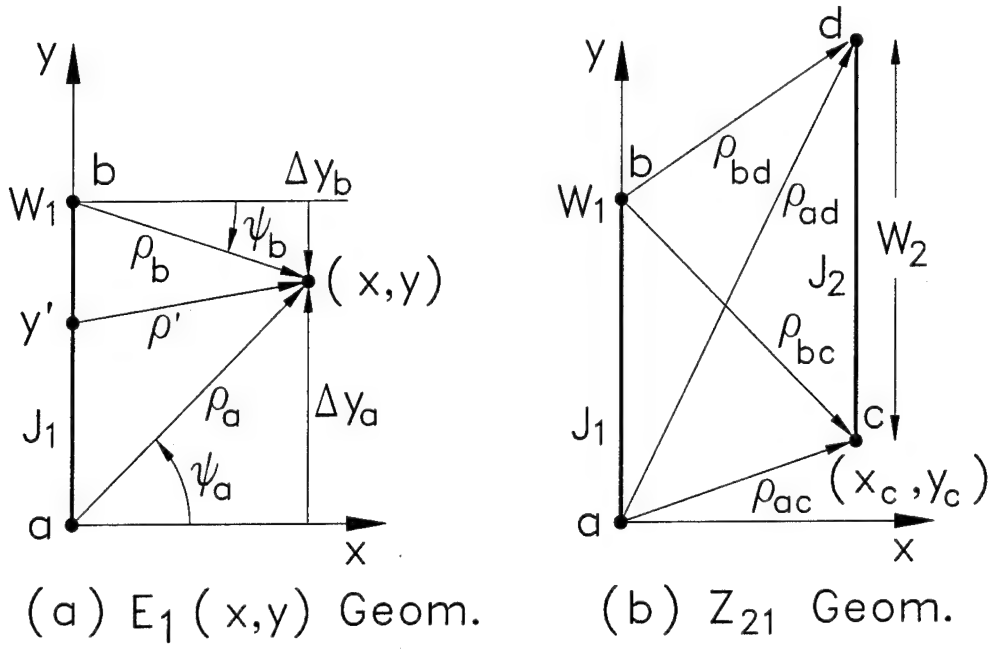

Figure A.1: Geometry for the computation of (a) $E_1(x,y)$ and (b) parallel Z_{21}.

$$\psi_{a,b} = \tan^{-1}\frac{\Delta y_{a,b}}{x} \qquad -\pi/2 \le \psi_{a,b} \le \pi/2 \tag{A.6}$$

are the distances and angles from ends a and b to the field point. Note that E_1 is finite at all (x,y). Using Maxwell's equations, the magnetic field associated with the electric field of Equation (A.4) is

$$\mathbf{H}_1(x,y) = \frac{-1}{j\omega\mu_0}\nabla \times \hat{\mathbf{z}}E_1 = \frac{1}{2\pi}\left[\hat{\mathbf{x}}\ln\frac{\rho_b}{\rho_a} + \hat{\mathbf{y}}(\psi_b - \psi_a)\right] \tag{A.7}$$

which has logarithmic singularities at ends a and b.

Inserting $E_1(x_c,y)$ from Equation (A.4) into (A.1) and integrating [25], the mutual impedance between Strips 1 and 2 is

$$Z_{21} \approx -CW_1W_2 - j\frac{2C}{\pi}[(F_{bd} - F_{bc}) - (F_{ad} - F_{ac})] \tag{A.8}$$

where

$$F_{ij} = \frac{1}{2}\rho_{ij}^2 \ln b\rho_{ij} - \frac{3}{4}\Delta y_{ij}^2 + x_c\Delta y_{ij}\psi_{ij} - \frac{x_c^2}{2}\ln\left[1 + \left(\frac{\Delta y_{ij}}{x_c}\right)^2\right] \tag{A.9}$$

in which Δy_{ij} is the y coordinate of end $j = c,d$ of Strip 2 with respect to end $i = a,b$ of Strip 1, i.e.,

$$\Delta y_{ac} = y_c, \quad \Delta y_{ad} = y_c + W_2, \quad \Delta y_{bc} = y_c - W_1, \quad \Delta y_{bd} = y_c + W_2 - W_1 \tag{A.10}$$

ρ_{ij} is the distance from end $i = a, b$ of Strip 1 to end $j = c, d$ of Strip 2, i.e.,

$$\rho_{ij} = \sqrt{x_c^2 + \Delta y_{ij}^2}. \tag{A.11}$$

and ψ_{ij} is the angle of the line from point i to point j with respect to the $+x$ axis, i.e.,

$$\psi_{ij} = \tan^{-1} \frac{\Delta y_{ij}}{x_c}. \tag{A.12}$$

For self impedances, $x_c = y_c = 0$ and $W_2 = W_1$. In this case, $F_{ac} = F_{bd} = 0$, and

$$F_{ad} = F_{bc} = \frac{1}{2} W_1^2 \ln bW_1 - \frac{3}{4} W_1^2. \tag{A.13}$$

Inserting Equation (A.13) into (A.8), the self impedance of Strip 1 is

$$Z_{11} \approx -CW_1^2 \left[1 - j \frac{2}{\pi} \left(\ln bW_1 - \frac{3}{2} \right) \right]. \tag{A.14}$$

In the evaluation of the self impedance for the trapezoidal cell of Figure 2.2(b), it is desirable to have a simplified version of Equation (A.8), so that the double integral of Equation (2.18) can be obtained in closed form. For Strips 1 and 2 within a trapezoidal cell whose thickness T is much less than its width W_n, $|x_c|, |y_c| \ll W_{1,2}$ and $W_2 \approx W_1$. In this case, dropping second order terms in x_c and y_c, $F_{ac} \approx 0 \approx F_{bd}$, and

$$F_{ad} = \frac{\pi}{2} W_2 |x_c| - \frac{3}{4} W_2^2 - W_2 y_c + \frac{1}{2} (W_2^2 + 2W_2 y_c) \ln bW_2 \tag{A.15}$$

$$F_{bc} = \frac{\pi}{2} W_1 |x_c| - \frac{3}{4} W_1^2 + W_1 y_c + \frac{1}{2} (W_1^2 - 2W_1 y_c) \ln bW_1. \tag{A.16}$$

Inserting Equations (A.15) and (A.16) into (A.8) and dropping second order terms yields

$$\begin{aligned} Z_{21} \approx & -CW_1 W_2 + j \frac{2C}{\pi} \left[\frac{\pi}{2} (W_1 + W_2) |x_c| - \frac{3}{4} (W_1^2 + W_2^2) \right. \\ & + \left. \frac{1}{2} W_2^2 \ln bW_2 + \frac{1}{2} W_1^2 \ln bW_1 \right]. \end{aligned} \tag{A.17}$$

Letting $W_2 = W_1 + \Delta W$ ($|\Delta W| \ll W_{1,2}$), Equation (A.17) becomes

$$Z_{21} \approx Z_{11} - CW_1 \Delta W + j \frac{2C}{\pi} [\pi W_1 |x_c| - W_1 \Delta W + W_1 \Delta W \ln bW_1] \tag{A.18}$$

in which the mutual impedance between Strips 1 and 2 is written as the self impedance of Strip 1 (Equation (A.14)) plus small correction terms.

Appendix B

Mutual Impedance Between General Skew Strips

This appendix will present approximate closed form expressions for the mutual impedance between general skew strips. Without loss of generality, Figure B.1 shows Strip 1 of width W_1 located along the $+y$ axis. Strip 2 is of width W_2 and extends from (x_c, y_c) at an angle ψ $(-\pi < \psi \leq \pi)$ with respect to the $+x$ axis. Both strips have unit surface current, i.e., $J_1 = J_2 = 1$ A/m. An arbitrary point (x, y) on Strip 2 can be described by the parametric equations

$$x = x_c + l\cos\psi, \quad y = y_c + l\sin\psi \qquad 0 \leq l \leq W_2. \tag{B.1}$$

The mutual impedance between expansion current J_1 and weighting current J_2 is

$$Z_{21} = -\int_0^{W_2} E_1(l) J_2 \, dl. \tag{B.2}$$

where E_1 is the free space electric field of J_1.

Inserting the ELF approximation for E_1 of Equation (A.4) into (B.2) and integrating yields

$$\begin{aligned} Z_{21} \approx & -CW_1W_2 - j\frac{2C}{\pi}\{[S(l = W_2, x_c, y_c - W_1, \psi) - S(l = 0, x_c, y_c - W_1, \psi)] \\ & -[S(l = W_2, x_c, y_c, \psi) - S(l = 0, x_c, y_c, \psi)]\} \end{aligned} \tag{B.3}$$

in which the S integral

$$S(l, x_c, y_c, \psi) = S_{ln}(l, x_c, y_c, \psi) - S_y(l, y_c, \psi) + S_{it}(l, x_c, y_c, \psi) \tag{B.4}$$

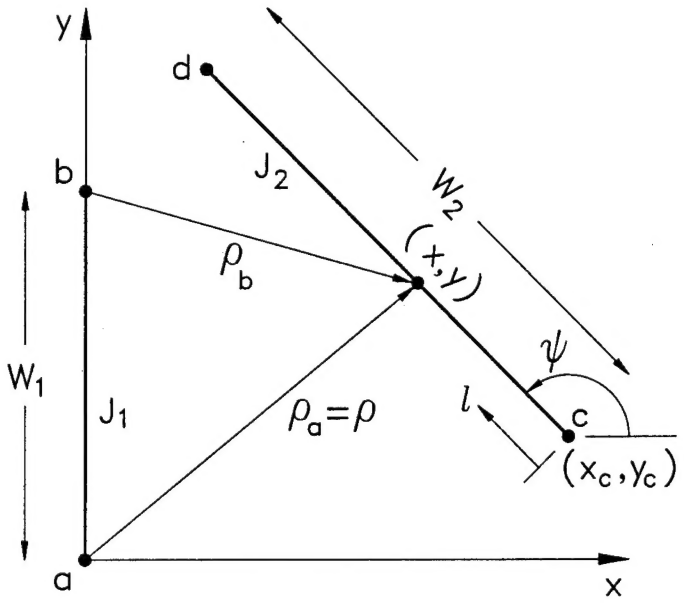

Figure B.1: Geometry for the computation of the mutual impedance between general skew strips.

is written as the sum of the S_{ln}, S_y, and S_{it} integrals.

The S_{ln} integral is defined by

$$S_{ln} = \int y \ln b\rho \, dl = S_1(l, x_c, y_c, \psi) + S_2(l, x_c, y_c, \psi) \tag{B.5}$$

$$\begin{aligned}
S_1(l, x_c, y_c, \psi) &= \frac{\sin\psi}{4b^2}[w^2 \ln w^2 - u^2] \\
S_2(l, x_c, y_c, \psi) &= \frac{y_c \cos^2\psi - x_c \cos\psi \sin\psi}{2b}[u \ln w^2 - 2u + 2v \tan^{-1}\frac{u}{v}] \\
u &= b[l + (x_c \cos\psi + y_c \sin\psi)] \quad b = 0.8905 k_0 \\
v &= b(y_c \cos\psi - x_c \sin\psi) \\
w^2 &= u^2 + v^2.
\end{aligned} \tag{B.6}$$

The S_y integral is defined by

$$S_y(l, y_c, \psi) = \int y \, dl = y_c l + \frac{\sin\psi}{2} l^2. \tag{B.7}$$

The S_{it} integral is defined by [1]

$$S_{it}(l, x_c, y_c, \psi) = \int x \tan^{-1} \frac{y}{x}\, dl = \cos\psi K_1(l, a, b, c, d) + x_c K_2(l, a, b, c, d) \qquad \text{(B.8)}$$

with $a = \sin\psi$, $b = y_c$, $c = \cos\psi$, $d = x_c$, and

$$K_1(l, a, b, c, d) = \int l \tan^{-1} \frac{al + b}{cl + d} dl = \qquad \text{(B.9)}$$
$$\left[\tan^{-1} \frac{al + b}{cl + d}\right] \left[\frac{l^2}{2} + \frac{X^2}{2Z^2}\right]$$
$$-\frac{X}{2Z}\left\{l - \frac{Y}{Z} \ln\left[\left(l + \frac{Y}{Z}\right)^2 + \frac{X^2}{Z^2}\right] + \frac{Y^2}{Z|X|} \tan^{-1}\left[\frac{lZ + Y}{|X|}\right]\right\}$$

in which

$$X = ad - bc, \quad Y = ab + cd, \quad Z = a^2 + c^2. \qquad \text{(B.10)}$$

$$K_2(l, a, b, c, d) = \int \tan^{-1} \frac{al + b}{cl + d} dl = \qquad \text{(B.11)}$$
$$\left[\tan^{-1} \frac{al + b}{cl + d}\right] \left[l + \frac{Y}{Z}\right] - \frac{X}{2Z} \ln[(al + b)^2 + (cl + d)^2].$$

If Equations (B.9) or (B.11) are used to perform a definite integral from l_1 to l_2, and if the path of integration crosses the branch of the $\tan^{-1}()$ function, i.e., $l_1 < -d/c < l_2$, then the following correction terms must be added to the definite integrals

$$-\frac{\pi}{2}\left[\frac{d^2}{c^2} + \frac{X}{Z^2}\right] \text{ for } \int_{l_1}^{l_2} l \tan^{-1} \frac{al + b}{cl + d} dl \qquad \text{(B.12)}$$

$$\pi \frac{aX}{cZ} \text{ for } \int_{l_1}^{l_2} \tan^{-1} \frac{al + b}{cl + d} dl. \qquad \text{(B.13)}$$

[1]The authors with to thank Mr. Ibrahim Tekin for the evaluation of the inverse tangent integrals, including the branch correction terms.

Bibliography

[1] K. Fitzgerald, M. G. Morgan, and I. Nair, "Electromagnetic Fields: the Jury's Still Out," IEEE Spectrum, Vol. 18, No. 8, pp. 22-35, August 1990.

[2] J. A. Stratton, Electromagnetic Theory, McGraw-Hill Book Company, Inc., New York, 1941. pp. 504, pp.511-513.

[3] S. A. Schelkunoff, Electromagnetic Waves, Princeton, N.J.: Van Nostrand, 1943, pp. 223-225, pp. 303-306.

[4] J. R. Moser, "Low-Frequency Low Impedance Electromagnetic Shielding" IEEE Transactions on Electromagnetic Compatability, Vol. EMC-30, No. 3, pp. 202-210, August 1988.

[5] S. Levy, "Electromagnetic Shielding Effect of an Infinite Plane Conducting Sheet Placed Between Circular Coaxial Cables," Proceedings of the IRE, Vol. 21, pp. 923-941, June 1936.

[6] J. C. Negi, "Radiation Resistance of a Vertical Dipole Over an Inhomogeneous Earth," Geophysics, Vol. 26, No. 5, pp. 635-642, April 1961.

[7] "Special Issue on Electromagnetic Shielding," IEEE Transactions on Electromagnetic Compatability, Vol. EMC-30, No. 3, pp. 185-341, August 1988.

[8] R. B. Schultz, V. C. Plantz, and D. R. Brush, "Shielding Theory and Practice," IEEE Transactions on Electromagnetic Compatability, Vol. EMC-30, No. 3, pp. 187-201, August 1988.

[9] J. E. Bridges, "An Update on the Circuit Approach to Calculate Shielding Effectiveness," IEEE Transactions on Electromagnetic Compatability, Vol. EMC-30, No. 3, pp. 211-221, August 1988.

[10] H. Wheeler, "The Spherical Coil as Inductor, Shield, or Antenna," Proceedings of the IRE, pp. 1595-1602, 1958.

[11] L. Hasselgren, E. Moller, and Y. Hamnerius, "Calculation of Magnetic Shielding of a Substation at Power Frequency Using FEM", IEEE Power Engineering Society 1994 Winter Meeting, New York, Jan. 30 - Feb. 3 1994.

[12] R.F. Harrington, *Field Computation by Moment Methods*, Krieger, Malarbar FL, 1982.

[13] M.R. Kragalott, "Physical Basis Method of Moments Analysis of Transverse Magnetic Shielding by Conducting Cylinders at Extremely Low Frequencies," Ohio State University, PhD dissertation, 1993.

[14] J.H. Richmond, "Scattering by a Dielectric Cylinder of Arbitrary Cross Section Shape," IEEE Trans. on Antennas and Prop., Vol. 13, pp. 338-341, May 1965.

[15] M. Kragalott and E.H. Newman, "A User's Manual for the General Cylinder Code (GCYL)," Ohio State Univ., ElectroScience Lab report 722644-1, prepared under contract PO D55951 with Rosemount, Inc., June 1990.

[16] J.H. Richmond, "Scattering by Thin Dielectric Strips,", IEEE Trans. on Antennas and Prop., Vol. 33, pp. 64-68, Jan. 1985.

[17] R.F. Harrington, *Time-Harmonic Electromagnetic Fields*, McGraw-Hill, New York, 1961.

[18] C.A. Balanis, *Advanced Engineering Electromagnetics*, John Wiley & Sons, New York, 1989.

[19] K.R. Demarest and R.J. Garbacz, "Anomalous Behavior of Near Fields Calculated by the Method of Moments," IEEE Trans. on Antennas and Prop., Vol. AP-27, pp. 609-614, Sep. 1979.

[20] J. Van Bladel, *Electromagnetic Fields*, Hemisphere, New York, 1985, Sec. 12.4.

[21] A. Frenkel, "On Entire Domain-Basis Functions with Square-Root Edge Singularity", IEEE Trans. on Antennas and Prop., Vol. AP-37, pp. 1211-1214, Sept. 1989.

[22] J.H. Richmond, "On the Edge Mode in the Theory of TM Scattering by a Strip or Strip Grating," IEEE Trans. on Antennas and Prop., Vol. AP-28, pp 883-887, Nov., 1980.

[23] D.R. Wilton and S. Govind, "Incorporation of Edge Conditions in Moment Method Solutions," IEEE Trans. on Antennas and Prop., Vol. AP-25, pp. 845-850, Nov. 1977.

[24] M. Abramowitz and I.A. Stegun, *Handbook of Mathematical Functions*, National Bureau of Standards, Applied Mathematics Series 55, 1970, Ch. 9.

[25] I.S. Gradshteyn and I.M. Ryzhik, *Table of Integrals Series and Products*, Academic Press, New York, 1980, Sec. 2.733.